Correspondence

Disseminated cutaneous *Mycobacterium kansasii* infection in an patient infected with the human immunodeficiency virus

People infected with the human immunodeficiency virus (HIV) are at a greater risk of mycobacterial infection and more than half of HIV-infected patients in developing countries are co-infected with mycobacteria. Therefore, mycobacterial infection is an important life-threatening complication in patients with HIV. In addition, immuno-compromised hosts with both tuberculosis and nontuberculous mycobacterial infections often show atypical clinical features, which can make it difficult for clinicians to make a precise diagnosis. We report a case of *Mycobacterium kansasii* infection in an patient with acquired immunodeficiency syndrome (AIDS) who developed extensive, cutaneous nodules and ulcers without any sign of pulmonary involvement.

A 34-year-old woman was referred to our dermatology clinic with an 8-month history of high fever and disseminated subcutaneous nodules and skin ulcerations.
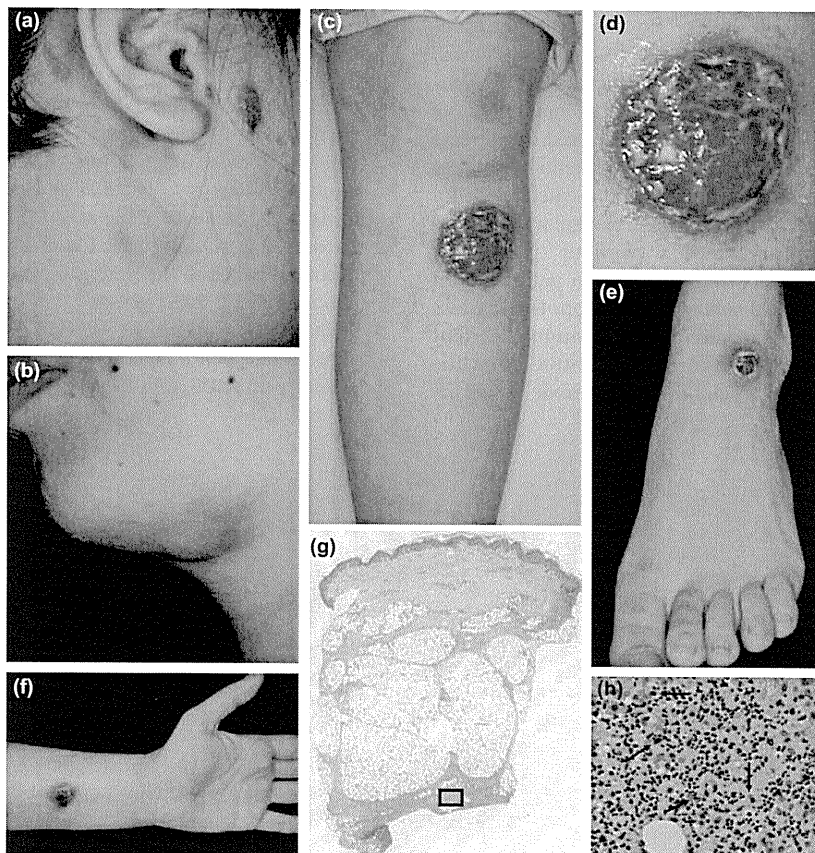

Figure 1 (a, b) Tender erythematous subcutaneous nodules scattered over the patient's neck and face; (c–f) skin ulcers on (c, d) the left lower thigh, (e) ankle and (f) forearm. (g, h) Large infiltrates of neutrophils associated with nontuberculous epithelioid granuloma (arrows). Haematoxylin and eosin; original magnification (g) × 2; (h) × 400.

1

On physical examination, subcutaneous nodules, up to 60 mm in size, scattered over her face (Fig. 1a) and limbs. On the lower left thigh, ankle and forearm, cutaneous ulcers, 20–40 mm in size were seen (Fig. 1b,c).

Histopathological examination of a biopsy taken from a nodule on the left forearm showed a large infiltrate of neutrophils associated with nontuberculous granuloma (Fig. 1d). Ziehl–Neelsen stain showed numerous acid-fast bacilli, which were confirmed as M. kansasii by DNA hybridization studies.

Results of laboratory investigations showed that the patient was positive for HIV-1, and her peripheral CD4 cell count was zero. Systemic examination showed extracutaneous signs of M. kansasii infection, including pulmonary nontuberculous mycobacteriosis.

The patient was treated with isoniazid 300 mg/day, ethambutol 750 mg/day, rifampin 450 mg/day and clarithromycin 800 mg/day, which resulted in gradual improvement. One month after beginning antimycobacterial treatment, the patient was started on highly active antiretroviral treatment.

M. kansasii is a slowly growing species that usually inhabits water supplies, swimming pools and sewage, and seldom infects healthy people.[1] However, immunosuppressed patients are often infected with M. kansasii, which usually causes pulmonary infection. Cutaneous M. kansasii infection is very rare and importantly, most cases of cutaneous M. kansasii infection have occurred in patients who are immunocompromised due to chemotherapy or immunosuppressive therapy for conditions such as autoimmune disease, renal or cardiac transplantations.[2,3] Cutaneous M. kansasii infection without pulmonary involvement has been reported in only two patients with AIDS, who both a showed solitary skin lesion. One patient had an asymptomatic ulcerative lesion around the right inguinal fold and the other had abscess formation on the thigh associated with regional lymph-node enlargement.[4,5] Our patient differs from these previous reports in that she had severe disseminated skin lesions, probably due to the considerably reduced number of peripheral blood CD4 cells.

The population of people infected with HIV has been increasing annually worldwide. In addition to the commonly observed nontuberculous mycobacterial infections with Mycobacterium avium and Mycobacterium intracellulare, clinicians should consider other uncommon mycobaceterial species such as M. kansasii, in order to ensure prompt and appropriate treatment for patients with HIV.

Y. Nomura, W. Nishie, A. Shibaki, M. Ibata and H. Shimizu
Department of Dermatology and Haematology, Hokkaido University
Graduate School of Medicine, Japan
E-mail: yukira0423@yahoo.co.jp
Conflict of interest: none declared.
Accepted for publication 22 June 2008

References

1 Stengem J, Grande KK, Hsu S. Localized primary cutaneous Mycobacterium kansasii infection in an immunocompromised patient. J Am Acad Dermatol 1999; 41: 854–6.

2 Tzen CY, Chen TL, Wu TY et al. Disseminated cutaneous infection with Mycobacterium kansasii: genotyping versus phenotyping. J Am Acad Dermatol 2001; 45: 620–4.

3 Patel R, Roberts GD, Keating MR et al. Infections due to nontuberculous mycobacteria in kidney, heart, and liver transplant recipients. Clin Infect Dis 1994; 19: 263–73.

4 Curco N, Pagerols X, Gomez L et al. Mycobacterium kansasii infection limited to the skin in a patient with AIDS. Br J Dermatol 1996; 135: 324–6.

5 Stellbrink HJ, Koperski K, Albrecht H et al. Mycobacterium kansasii infection limited to skin and lymph node in a patient with AIDS. Clin Exp Dermatol 1990; 15: 457–8.

QUIZ SECTION

Progressive Refractory Ulcer of the Nipple: A Quiz

Yukiko Nomura, Masashi Akiyama, Wataru Nishie and Hiroshi Shimizu
Department of Dermatology, Hokkaido University Graduate School of Medicine, N15 W7, Sapporo 060-8638, Japan. E-mail: yukira0423@yahoo.co.jp

A 50-year-old woman presented with erosive erythema and effusion on the right nipple one year previously, which gradually became ulcerated and painful. One month after the initial presentation, the ulcer was excised by a breast surgeon. Histopathological examination of the resected tissue revealed non-specific inflammation with no evidence of malignancy. The wound healed completely, but an ulcer reappeared at the same site 3 months later. The same surgical operation was performed again and the wound healed, but the ulcer reappeared 2 months after that operation.

More than 6 months later the patient was finally referred to our hospital with an ulcer on the right breast. Examination revealed an ulcer approximately 3 cm in diameter in the right areola (Fig. 1). Bacterial, fungal and mycobacterial cultures from the ulcer were all negative. Histopathological observations of a skin biopsy from the edge of the ulcer showed necrosis of the epidermis forming the ulcer, and mixed inflammatory cell infiltrate with abscess formation at the base of the ulcer. The patient had been healthy except for hyperlipidaemia and a liver cyst.

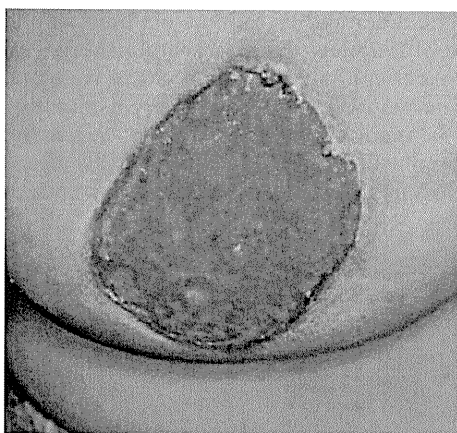*What is your diagnosis?* See next page for answer.

Fig. 1. Painful ulcer of the right nipple.

doi: 10.2340/00015555-0678

Progressive Refractory Ulcer of the Nipple: Comment

Diagnosis: **Pyoderma gangrenosum**

At first, severe mastitis and invasive breast cancer were considered as a differential diagnosis for pyoderma gangrenosum (PG) of the breast.

The patient was treated with oral prednisolone, 0.5 mg/day/kg, topical corticosteroid ointment applied to the right side of the ulcer and tacrolimus ointment applied to the left side of the ulcer. Her pain diminished dramatically, and the ulcer epithelialized on both the right and the left sides. The wound healed completely 6 months after the start of the medication, at which time the patient stopped taking prednisolone (Fig. 2). Nine months after stopping the prednisolone, there has been no recurrence.
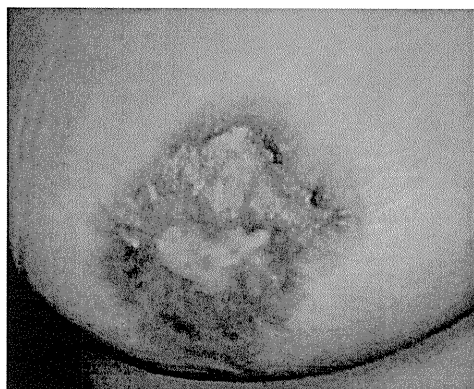

Fig. 2. Complete healing after 6 months of systemic corticosteroid treatment.

PG is a relatively rare non-infectious neutrophilic dermatosis induced by minor skin trauma or underlying systemic disorders (1, 2). For early and mild PG lesions, several kinds of treatment, including topical or intralesional corticosteroids or topical tacrolimus, are reported to be effective (2). Systemic corticosteroids and/or cyclosporine appear to be effective in most cases and should be considered as the first-line therapy (3).

PG can affect any site of the body, but it is most common in the lower limbs. However, its occurrence on the breast is extremely rare. To our knowledge, only 28 cases of PG on the breast have been reported, 22 of which developed after injury, skin biopsy or operation such as mammaplasty (4). To our knowledge, only one case of PG of the breast without any skin trauma or underlying systemic disease has been reported previously (5).

REFERENCES

1. Harris AJ, Regan P, Burge S. Early diagnosis of pyoderma gangrenosum is important to prevent disfigurement. BMJ 1998; 316: 52–53.
2. Callen JP. Pyoderma gangrenosum and related disorders. Med Clin North Am 1989; 73: 1247–1261.
3. Reichrath J, Bens G, BonowitzA, Tilgen W. Treatment recommendations for pyoderma gangrenosum: an evidence-based review of the literature based on more than 350 patients. J Am Acad Dermatol 2005; 53: 273–283.
4. Bonamigo RR, Behar PR, Beller C, Bonfá R. Pyoderma gangrenosum after silicone prosthesis implant in the breasts and facial plastic surgery. Int J Dermatol 2008; 47: 289–291.
5. Harries MJ, McMullen E, Griffiths CE. Pyoderma gangrenosum masquerading as dermatitis artefacta. Arch Dermatol 2006; 142: 1509–1510.

Delayed contralateral hemiplegia or hemiparesis has been rarely reported as a complication of herpes zoster ophthalmicus.[3] However, there were two suggested causes of this complication. Firstly, the VZV spread directly along the intracranial branches of the trigeminal nerve to the ipsilateral arterial walls via the afferent trigeminal ganglionic fibres.[2,4] Secondly, the inflammatory process spread from the trigeminal ganglion to nearby blood vessels, leading to thrombosis and distal embolization.[3]

PCR analysis of CSF is a specific and sensitive test for VZV detection and is the mainstay for diagnosing the neurological complications of VZV infection in patients.[2] Intravenous aciclovir for 10–14 days is recommended in adults with VZV arteritis.[5] Our patient was an immunocompetent middle-aged man with herpes zoster and zoster ophthalmicus complicated by meningitis and delayed ipsilateral ICH even though he was treated appropriately with intravenous aciclovir. In general, there are two main mechanisms of the ICH related to infection or inflammation; rupture of an intracranial aneurysm or cerebral venous sinus thrombosis.[5] However, our patient had no evidence of an intracranial aneurysm or of venous sinus pathology on the CT angiogram.

To our knowledge, this is the first report of herpes zoster complicated by delayed ICH in the dermatology literature, although there are a few reports of ICH complicating herpes zoster in the medical literature of other fields of study.

H.-J. Song, W.-K. Hong, H.-S. Lee, G.-S. Choi and J.-H. Shin
*Department of Dermatology, Inha University School of Medicine,
7-206 shinhung-dong-3-ka, Jung-ku, Incheon, 400-711, Republic of
Korea*
E-mail: jshin@inha.ac.kr
Conflict of interest: none declared.
Accepted for publication 3 April 2008

References

1 Jain R, Deveilis J, Hickenbottom S, Mukherji SK. Varicella-zoster vasculitis presenting with intracranial hemorrhage. *Am J Neuroradiol* 2003; **24**: 971–4.
2 Kleinschmidt-Demasters BK, Gilden DH. Varicella-zoster virus infections of the nervous system: clinical and pathologic correlates. *Arch Pathol Lab Med* 2001; **125**: 770–80.
3 Mackenzie RA, Ryan P, Karnes WE, Okazaki H. Herpes zoster arteritis: pathological findings. *Clin Exp Neurol* 1987; **23**: 219–24.
4 Hilt DC, Buchholz D, Krumholz A *et al.* Herpes zoster ophthalmicus and delayed contralateral hemiparesis caused by cerebral angitis: diagnosis and management approaches. *Ann Neurol* 1983; **14**: 543–53.
5 Danchaivijitr N, Miravet E, Saunder DE *et al.* Post-varicella intracranial hemorrhage in a child. *Dev Med Child Neurol* 2006; **48**: 139–42.

Widespread keratosis follicularis squamosa

Keratosis follicularis squamosa (KFS), first described by Dohi and Momose in 1903,[1] is characterized by small, scattered, scaly lesions up to 10 mm in diameter with tiny pigmented keratotic plugs in the centre. We describe a case of KFS that involved extraordinarily large areas of the body.

A 42-year-old Japanese woman presented with a 2-year history of a symmetrical, scaly eruptions over her body, extending to the legs (Fig. 1a–c). She had been treated with topical corticosteroid ointments for >1 year. She had also

Figure 1 (a) Distribution of lesions involving the axilla, buttocks, lower abdomen, the posterior thighs and lower legs; (b,c) small scattered scaly patches up to 10 mm in diameter with small pigmented keratotic plugging in the centre seen on (b) the lower axilla and (c) buttocks; (d) the margin of each scale was slightly detached from the plaques. (e) Dermatoscopy shows brown dots in the centre associated with hair follicles, but no pigment network was seen.
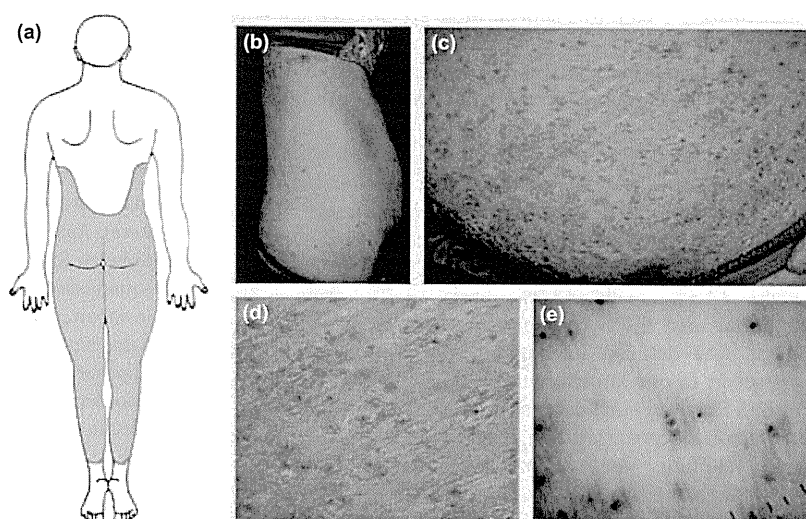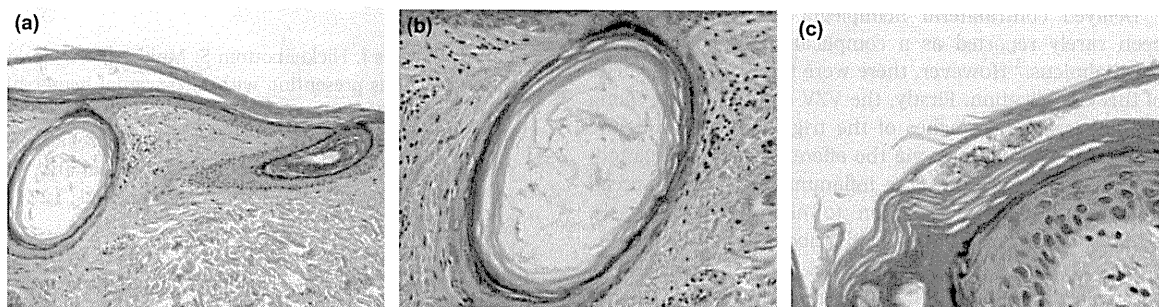
Figure 2 (a–c) Dilated hair follicles with keratotic plugging and separated horny layer from epidermis at the periphery (haematoxylin and eosin; original magnification × 100); bacterial structures were seen in (b) dilated hair follicle and (c) horny layers.

been taking various drugs (chlorpromazine hibenzate, etizolam, flunitrazepam, triazolam and promethazine methylene disalicylate) for 10 years to treat depression. There was no family history of note.

Physical examination revealed small, scattered, scaly lesions up to 10 mm in diameter with tiny pigmented keratotic plugs in the centre (Fig. 1d,e). The margin of each scale was slightly detached from the plaques.

Dermoscopic observation revealed brown dots in the centre of each lesion associated with hair follicles. Laboratory examinations, including measurement of oestrogen, progesterone and prolactin levels, showed no abnormalities.

Histopathological examination of a biopsy taken from a lesion showed hyperkeratosis without parakeratosis, dilated hair follicles with keratotic plugging, and a horny layer separated from the epidermis at the periphery of the lesion (Fig. 2a). Bacterial debris-like material was observed in the dilated hair follicle (Fig. 2b) and horny layers (Fig. 2c). Staining with periodic-acid–Schiff did not reveal any fungal structures. No specific changes were observed in the dermis.

A diagnosis of KFS was made. Topical application of moisturizing cream (0.3% heparinoid cream) to the lesions was effective and led to the clinical disappearance of the majority of the lamellar scaling within 1 year, but some tiny pigmented papules remained on the patient's buttocks and thighs.

Yajima et al. reviewed 201 Japanese patients with KFS.[2] According to their review, KFS occurred predominantly in the third and fourth decades of life, with a male : female ratio of 1 : 1.6. The distribution of the affected sites was restricted: abdomen 53.7%, thighs 35.1%, buttocks 34.5%, waist 33.5%, axilla 32.9%, back 12.7%, arms 5.3%, inguinal area 4.7% and lower legs 3.7%, in 188 cases there was detailed information of the affected areas. However, to our knowledge, no previously reported cases of KFS involved such extensive areas as our patient.

Hereditary predisposition, bacterial infection, irritation from clothing, and hormonal imbalance have been proposed as pathogenic factors, although these factors fail to explain the exact pathogenesis of this abnormal keratinization.[3] In some cases, Gram-positive cocci have been observed in the central plugging in the hair follicles.[4] In our patient, continuous long-term topical corticosteroid therapy might have caused the proliferation of bacteria and contributed to the build-up of bacterial material in the dilated hair follicle and horny layers, and led to this peculiar clinical feature.

To date, as many as 245 Japanese cases of KFS have been described, but only three cases have been reported in other countries (China, Korea and Russia).[5] Although KFS is a well-known disease in Japan, it has not been widely reported in the English literature. Additional cases of this skin disorder from other ethnic groups should clarify the prevalence and pathogenesis of KFS.

Y. Nomura, M. Abe, K. Natsuga, R. Moriuchi, H. Kawasaki, M. Mayuzumi, A. Yasuoka* and H. Shimizu
Department of Dermatology, Hokkaido University Graduate School of Medicine, N15, W7, Sapporo 060–8638, Japan; and
*Yasuoka Dermatology Clinic, Sapporo, Japan
E-mail: deka-abe@med.hokudai.ac.jp
Conflict of interest: none declared.

References

1 Dohi K, Momose G. A presentation of patients with a certain follicular squamous keratosis (in Japanese). Jpn J Dermatol 1903; **3**: 513–14.
2 Yajima C, Kobayashi H, Ohkawara A. A case of keratosis follicularis squamosa (Dohi) following weight loss (in Japanese). Rinsho Derma (Tokyo) 1998; **40**: 1123–6.
3 Shimizu S, Shimizu T, Tateishi Y et al. Keratosis follicularis squamosa (Dohi): a follicular keratotic disorder well known in Japan. Br J Dermatol 2001; **144**: 1070–2.
4 Katayama I, Yokozeki O, Nishioka K. Oral minocycline improved ketatosis folicularis squamosa (Dohi) and related disorder: bacterial factors are possibly involved in aberrant keratinization. J Dermatol 1994; **21**: 604–8.
5 Lee S, Kim SC. A Korean case of keratosis follicularis squamosa (Dohi) successfully treated with roxithromycin. Br J Dermatol 2002; **29**: 676–7.

A Novel Humanized Neonatal Autoimmune Blistering Skin Disease Model Induced by Maternally Transferred Antibodies[1]

Wataru Nishie,[2]* Daisuke Sawamura,*[†] Ken Natsuga,* Satoru Shinkuma,* Maki Goto,* Akihiko Shibaki,* Hideyuki Ujiie,* Edit Olasz,[‡] Kim B. Yancey,[§] and Hiroshi Shimizu*

All mammal neonates receive maternal Abs for protection against pathogenic organisms in the postnatal environment. However, neonates can experience serious adverse reactions if the Abs transferred from the mother recognize self-molecules as autoAgs. In this study, we describe a novel model for autoimmune disease induced by transferred maternal Abs in genetically transformed Ag-humanized mice progeny. Bullous pemphigoid is the most common life-threatening autoimmune blistering skin disease that affects the elderly, in which circulating IgG autoAbs are directed against epidermal type XVII collagen (COL17). We have established a genetically manipulated experimental mouse model in which maternal Abs against human COL17 are transferred to pups whose skin expresses only human and not mouse COL17, resulting in blistering similar to that seen in patients with bullous pemphigoid. Maternal transfer of pathogenic Abs to humanized neonatal mice is a unique and potential experimental system to establish a novel autoimmune disease model. *The Journal of Immunology*, 2009, 183: 4088–4093.

D uring pregnancy and after birth, all mammal neonates receive various factors from their mothers to adapt to the new environment, including Abs for protection against pathogenic organisms (1, 2). However, this can result in serious adverse reactions in neonates if the transferred Abs recognize self-molecules as autoAgs. For example, neonatal lupus, which is clinically characterized by skin eruptions and fatal congenital heart block, is induced by autoAbs against Ro/SSA, Ro/SSB, or U1 ribonuclear protein transferred from mothers affected with Sjögren syndrome or systemic lupus erythematosus (3, 4). In addition, maternally transferred autoAbs against acetylcholine receptors can induce the characteristic features of myasthenia gravis in human neonates (5). This suggests that mothers, in experimental animal models, might be able to induce autoimmunity in their offspring.

One possible approach to using maternal Abs to produce disease models for autoimmune diseases is the use of gene-targeted mice (6). Immunizing Ag-knockout female mice with a targeted Ag can induce Abs against the antigenic molecule. Mating these immunized females with wild-type males could mimic autoimmune diseases in the neonates expressing antigenic peptides transcribed by paternal genes in the presence of circulating maternally transferred Ag-specific IgG (6). However, this approach has not achieved practical application, probably because gene-targeted mice often

die soon after birth, especially when the targeted genes encode functionally important proteins (7–11). Consequently, another method that does not use lethal gene-deleted maternal mice is desirable. The difference in immune systems between humans and mice is another important problem underlying most of the current experimental autoimmune disease models. In fact, the autoAgs in existing autoimmune disease models have been the mouse's own proteins, which are expected to differ from those in the human autoimmune disease condition (12–14). Therefore, autoimmune disease models with human autoAg expression would be ideal.

In this study, we tried to produce a novel neonatal autoimmune disease model induced by passage of maternal IgG. We aimed at the most common and life-threatening autoimmune blistering skin disease, bullous pemphigoid (BP).[3] In BP, circulating IgG autoAbs are directed against type XVII collagen (COL17, formerly known as BP180 or BPAG2) in the skin (15, 16). COL17 is a type-II-oriented, 180kD hemidesmosomal transmembrane protein that anchors basal keratinocytes to the underlying epidermal basement membrane. The pathogenic epitope in COL17 is tightly clustered within the noncollagenous (NC) 16A stretch of its ectodomain (17, 18). Interestingly, due to significant differences between humans and rodents in the amino acids sequence in the NC16A region, mice that have received human IgG from BP patients fail to show any clinical, histological, or immunological findings consistent with BP (13, 14). We recently generated *Col17a1* gene-targeted ($mCol17^{-/-}$) mice as well as COL17-humanized mice by introducing human $COL17A1$cDNA ($hCOL17^{+/+}$) transgene driven under keratin 14 promoter into $mCol17^{-/-}$ mice (12, 19). Importantly, the $mCol17^{-/-}$ mice were too fragile to mate with male mice, but reproductive ability was restored in COL17-humanized ($mCol17^{-/-}$, $hCOL17^{+/+}$) mice (12). In this study, we used these genetically manipulated COL17-humanized mice to produce a novel neonatal autoimmune disease model induced by passage of maternal IgG.

① Immunization of *mCol17⁺ᐟ⁻* female with human COL17

Skin sample obtained from human
COL17 Tg mouse was grafted.

♀ : *mCol17⁺ᐟ⁻, hCOL17⁻ᐟ⁻*

Mouse COL17 (+)
Human COL17 (-)

② Mating immunized *mCol17⁺ᐟ⁻* female with COL17-
humanized male mouse

♀ : *mCol17⁺ᐟ⁻, hCOL17⁻ᐟ⁻*   X   ♂ : *mCol17⁻ᐟ⁻, hCOL17⁺ᐟ⁺*

Mouse COL17 (+)   Mouse COL17 (-)
Human COL17 (-)   Human COL17 (+)

↓

pups {

mCol17⁺ᐟ⁻, hCOL17⁺ᐟ⁻
Mouse COL17 (+) Human COL17 (+)

→ Blistering skin disease
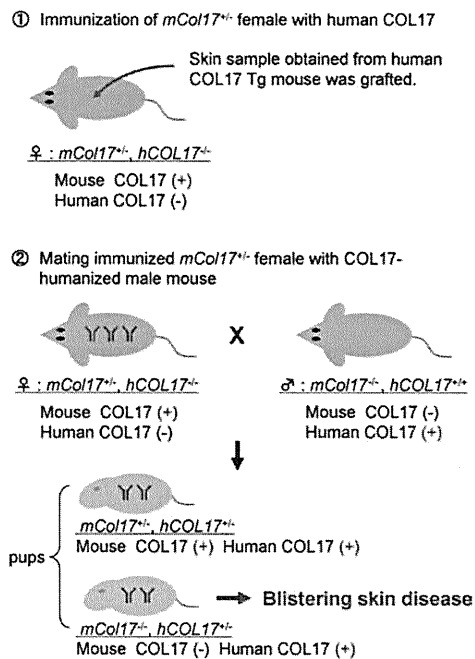
mCol17⁻ᐟ⁻, hCOL17⁺ᐟ⁻
Mouse COL17 (-) Human COL17 (+)
}

FIGURE 1. Schematic of the method for generating the neonatal BP model. Four-to 6-wk-old heterozygous *mCol17⁺ᐟ⁻* female mice (C57BL/6 background) were immunized against human COL17 by grafting skin obtained from gender-matched, syngeneic human COL17 cDNA Tg mouse driven under keratin 14 promoter (1). Two weeks after grafting, the immunized female mice were crossed with 6- to 8-wk-old COL17-humanized (*mCol17⁻ᐟ⁻, ʰCOL17⁺ᐟ⁺*) males. Theoretically, half of the newborns should express only human COL17 in the skin (*mCol17⁻ᐟ⁻, ʰCOL17⁺ᐟ⁻*), and these are expected to be a neonatal BP model (2).

Materials and Methods

Gross summary of strategy

We selected a breeding pair consisting of heterozygote *Col17a1*-deficient (*mCol17⁺ᐟ⁻*) female mice and COL17-humanized (*mCol17⁻ᐟ⁻, hCOL17⁺ᐟ⁺*) male mice (Fig. 1). Theoretically, half of the pups from this pair should express only human COL17 in the skin while the other half should express both mouse and human COL17 (Fig. 1). Wild-type mice can develop quite high titers of circulating anti-human COL17 IgG when grafted with human COL17 transgenic (Tg) mouse skin (19). We first immunized *mCol17⁺ᐟ⁻* mother mice with skin grafts obtained from human COL17 Tg mouse, and then we mated the immunized *mCol17⁺ᐟ⁻* mother mice with COL17-humanized (*mCol17⁻ᐟ⁻, hCOL17⁺ᐟ⁺*) male mice. Neonatal COL17-humanized (*mCol17⁻ᐟ⁻, hCOL17⁺ᐟ⁺*) mice retained skin stability against mechanical friction (12); similarly, neonatal COL17-humanized mice heterozygously carrying human COL17 cDNA transgene (*mCol17⁻ᐟ⁻, hCOL17⁺ᐟ⁻*) showed none of the skin abnormalities seen in *mCol17⁻ᐟ⁻* mice, although it was possible to detach the epidermis by moderate mechanical friction (our unpublished data). We hypothesized that immunized *mCol17⁺ᐟ⁻* mother mice would produce circulating anti-human COL17 IgG that would be transferred into their neonates including those whose skin expressed only human and not mouse COL17 (*mCol17⁻ᐟ⁻, hCOL17⁺ᐟ⁻*), resulting in natural blistering that replicates human BP disease (Fig. 1).

Immunization of the heterozygote mCol17⁺ᐟ⁻ female mice

Four- to 6-wk-old heterozygote-null *mCol17⁺ᐟ⁻* female mice (F₁ mouse was 129/SvEv × C57BL/6 background, back-crossed with C57BL/6 over 10 generations) were immunized against human COL17 as previously described (19), with minor modifications. In brief, 1 × 1 cm of back skin obtained from gender-matched, syngeneic human COL17 cDNA Tg mice was grafted onto the back of the recipient *mCol17⁺ᐟ⁻* female mice. As a control, back skin obtained from wild-type C57BL/6 was grafted onto recipient *mCol17⁺ᐟ⁻* female mice (n = 5). The grafted skin was sutured, and bandages were removed 7 days after skin grafting.

Generation of neonatal BP mice

Two weeks after skin grafting, the immunized and the control *mCol17⁺ᐟ⁻* female mice were crossed with 6- to 8-wk-old COL17-humanized (*mCol17⁻ᐟ⁻, hCOL17⁺ᐟ⁺*) male mice (12). Half of their newborns (*mCol17⁻ᐟ⁻, hCOL17⁺ᐟ⁻*) were predicted to express only human COL17 and not mouse COL17 in the skin and the other half of the newborns (*mCol17⁺ᐟ⁻, hCOL17⁺ᐟ⁻*) to express both mouse and human COL17 in the skin (Fig. 1).

Evaluation of serum anti-human COL17 IgG in the immunized mother mice and their neonates

Sera from immunized *mCol17⁺ᐟ⁻* females (before immunization and 1 to 4 wk after immunization) and their neonates (at birth and 1 to 4 wk after birth, respectively) were sampled, followed by ELISA and indirect immunofluorescence (IIF) to evaluate the circulating mouse IgG Abs directed against human COL17 (12, 19). The ELISA index value against the human COL17 NC16A domain peptide was measured using BP180 ELISA kit (MBL) with minor modifications. In brief, this kit is designed to detect human IgG against human COL17; therefore, HRP-conjugated goat polyclonal anti-mouse IgG (1/20,000 dilution, Jackson ImmunoResearch Laboratories) was used as a secondary Ab substitute for prepared HRP-conjugated anti-human IgG. The absorbance was measured at 450 nm by microtiter plate readers (Bio-Rad). For IIF studies, serum from the mice was serially diluted in PBS. Normal or 1M NaCl split human skin samples were obtained from a healthy volunteer and incubated with the sera for 30 min at 37°C, followed by staining with FITC-conjugated polyclonal goat anti-mouse IgG (1/100 dilution, Jackson ImmunoResearch Laboratories) as described previously (12, 19).

Immunopathological analysis of neonatal BP

For histological investigations, back skin of the mice was obtained at birth and 1 to 4 wk after birth, and processed for H&E staining and direct immunofluorescence (DIF) microscopy. For DIF study, FITC-conjugated goat polyclonal anti-mouse IgG (1/100 dilation, Jackson ImmunoResearch Laboratories), rat monoclonal anti-mouse IgG1, IgG2a, IgG2b (1/100 dilution, BD Pharmingen), goat polyclonal anti-mouse IgG2c (1/400 dilation, Bethyl Laboratories), and FITC-conjugated goat anti-mouse C3 (1/200 dilation, Cappel) were used (12, 14, 20).

Passive transfer of maternal IgG with or without immunoadsorption against human COL17 NC16A protein into neonatal COL17-humanized (mCol17⁻ᐟ⁻, hCOL17⁺ᐟ⁺) mice

Total IgG was purified from pooled sera obtained from 5 immunized *mCol17⁺ᐟ⁻* females (10 wks after skin grafting) using HiTrap Protein G HP (GE Healthcare) according to the manufactur's instructions. Recombinant human COL17 NC16A (amino acid: 490–566) protein was generated as a gulutathione S-transferase (GST) fusion protein as previously described (12), and 6 mg of the purified protein was coupled with 1 ml of GSTrap FF (GE Healthcare). Half of the purified total IgG was coupled with the human COL17 NC16A-GST protein in the column to eliminate Abs directing to human COL17 NC16A protein, and flow-through samples were collected. Total IgG with or without immunoadsorption using human COL17 NC16A protein were concentrated by Amicon Ultra-50 ultracentrifuge (Millipore), and each was adjusted to be 2.1 μg/μl. Fifty μl of Abs was i.p. injected into neonatal COL17-humanized (*mCol17⁻ᐟ⁻, hCOL17⁺ᐟ⁺*) mice as previously described (12).

All mouse procedures were approved by the Institutional Animal Care and Use Committee of Hokkaido University, and fully informed consent from all patients was obtained for the use of their materials.

Results

High titers of IgG Abs against human COL17 were induced in recipient mother mice and they were efficiently transferred to their neonates

Consistent with the previous report in which high titer of IgG against human COL17 were successfully induced when human COL17 Tg mouse skin was grafted onto the wild-type mice (19), the heterozygote *mCol17⁺ᐟ⁻* female mice also developed high titers of circulating anti-human COL17 IgG after skin grafting of human COL17 cDNA Tg mice skin (Fig. 2, a–c). ELISA studies clearly showed the presence of circulating anti-human COL17 IgG at 3 wk after skin grafting, and a maximum titer was reached at
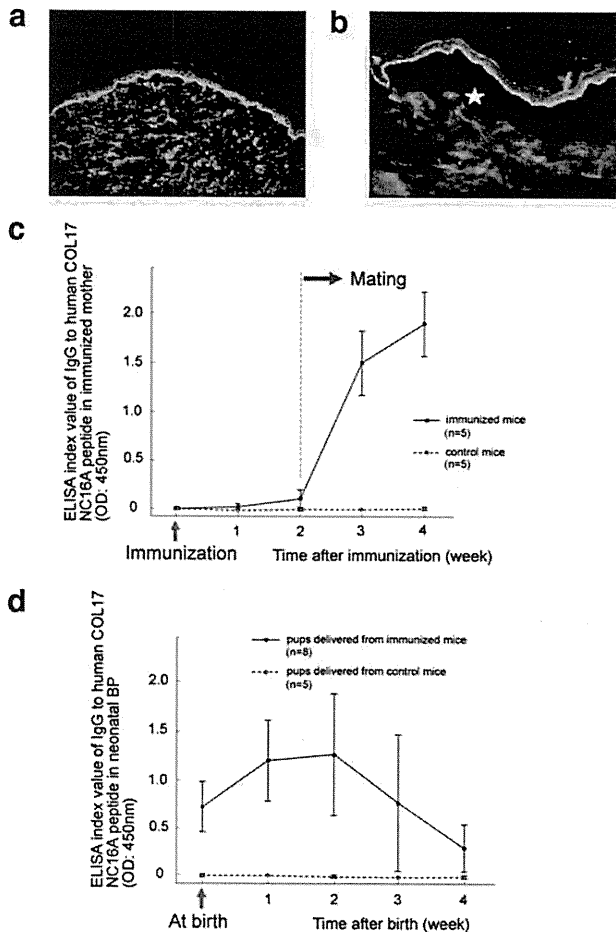
FIGURE 2. Profile of IgG Abs against human COL17 in immunized heterozygote $mCol17^{+/-}$ female and neonatal mice. *a*, IIF study using normal human skin as a substrate demonstrated the presence of IgG Abs against the dermal-epidermal junction in the sera of immunized mothers. *b*, These Abs reacted with the epidermal side of the basement membrane zone in skin incubated with 1M-NaCl (star shows cleft between epidermis and dermis). *c*, Heterozygous recipient $mCol17^{+/-}$ female mice developed high titers of circulating anti-human COL17 IgG around 3 wk after immunization. *d*, Maternal IgG was efficiently transferred into neonates, rapidly decreasing 2 to 3 wk after birth. The majority of maternal IgG had disappeared by 4 wk after birth.

4 wk (Fig. 2*c*). IIF study using 1M NaCl split normal human skin as a substrate demonstrated that this anti-human COL17 IgG reacted with the epidermal side of the basement membrane (Fig. 2*b*), consistent with the reactivity of human BP autoAbs (15, 16). We then crossed immunized heterozygous *Col17*-deficient ($mCol17^{+/-}$) female mice and COL17-humanized ($mCol17^{-/-}$, $hCOL17^{+/+}$) male mice to give birth to their neonates (Fig. 1). In the neonates delivered from these immunized female mice, maternally transferred IgG against human COL17 was retained at high titers for at least 2 wk after birth, after which it decreased, disappearing by 4 wk after birth (Fig. 2*d*). In the control, $mCol17^{+/-}$ female mice, which had been grafted with wild-type mice skin, no anti-human COL17 IgG Abs could be observed nor in their pus delivered after mating them with COL17-humanized ($mCol17^{-/-}$, $hCOL17^{+/+}$) male (Fig. 2, *c* and *d*).

Neonatal BP mice developed severe blistering

All ($n = 12$) of the neonatal BP mice that expressed only human COL17 and not the mouse ortholog in the skin with maternally

transferred IgG against human COL17 showed severe skin fragility and the epidermis easily detached with minor mechanical friction (Nikolsky phenomenon, Fig. 3*a*). Notably some mice developed spontaneous small blisters and pustules (Fig. 3, *a* and *c*). These skin lesions gradually disappeared in the first week after birth, leaving small, round, crusted lesions similar to those seen in BP patients (Fig. 3*b*). Although epidermal detachment could be induced by moderate (but not minor) friction in humanized mice heterozygously carrying the human COL17 cDNA transgene ($mCol17^{-/-}$, $hCOL17^{+/-}$), the skin fragility observed in neonatal BP mice was obviously more severe, and minor friction easily produced extensive epidermal detachment. In contrast, none of the other neonates ($n = 13$) that expressed both human and mouse COL17 in skin ($mCol17^{+/-}$, $hCOL17^{+/-}$) demonstrated any distinct skin abnormalities following exposure to maternal IgG, including spontaneous blister formation or Nikolsky phenomenon (data not shown).

Neonatal BP mice showed histological and immunological features identical with those seen in patients with BP

This system is characterized by complete humanization of the Ag in neonatal mice with ensuing inflammatory cascades that are completely mouse-derived. Therefore, the system is able to induce specific IgG-Ag reactions and lead to skin inflammation consistent with BP in humans. Notably, histological examinations demonstrated distinctive subepidermal blister formation with numerous inflammatory cell infiltrates predominately consisting of neutrophils (Fig. 3*c*). DIF studies of BP model mice skin revealed deposition of mouse IgG and of mouse complement (C3) in epidermal basement membrane until the third and the first to second weeks after birth, respectively (Fig. 3*d*). Subclass analysis of in vivo deposition of IgG showed that IgG1 and IgG2c predominated at the dermal-epidermal junction (Fig. 3*e*). This characteristic of IgG subclass deposition was the same for immunized $mCol17^{+/-}$ females as for their neonates, as shown by IIF on the normal human skin as a substrate (data not shown).

IgG Abs to the NC16A domain of human COL17 play a major role in inducing blistering skin disease

We previously demonstrated that IgG Abs to the NC16A domain of human COL17 play a major role in induce blistering disease; this was demonstrated by passive-transfer experiments using IgG autoAbs from BP patients in neonatal COL17-humanized ($mCol17^{-/-}$, $hCOL17^{+/+}$) mice (12). To assess and characterize the role of IgG Abs in immunized $mCol17^{+/-}$ female mice in the current model, we performed passive-transfer experiment using IgG Abs obtained from immunized female mice with or without immunoadsorption against human COL17 NC16A protein ($n = 2$, respectively). By IIF study using normal human skin as a substrate, both immune-adsorbed and without immunoadsorption purified IgG reacted to the dermal-epidermal junction until 5120 and 20480 times dilution respectively (data not shown). The passive-transfer experiment showed that purified total IgG without immunoadsorption with human COL17 NC16A protein resulted in skin fragility associated with IgG deposition along the dermal-epidermal junction (Fig. 4, *a* and *b*). In contrast, treatment of IgG with COL17 NC16A protein resulted in no blistering phenotype, although slight deposition of IgG could be observed along the dermal-epidermal junction (Fig. 4, *a* and *b*). These results clearly suggest that IgG Abs to NC16A domain of human COL17 played the major role to induce blistering skin disease in vivo.
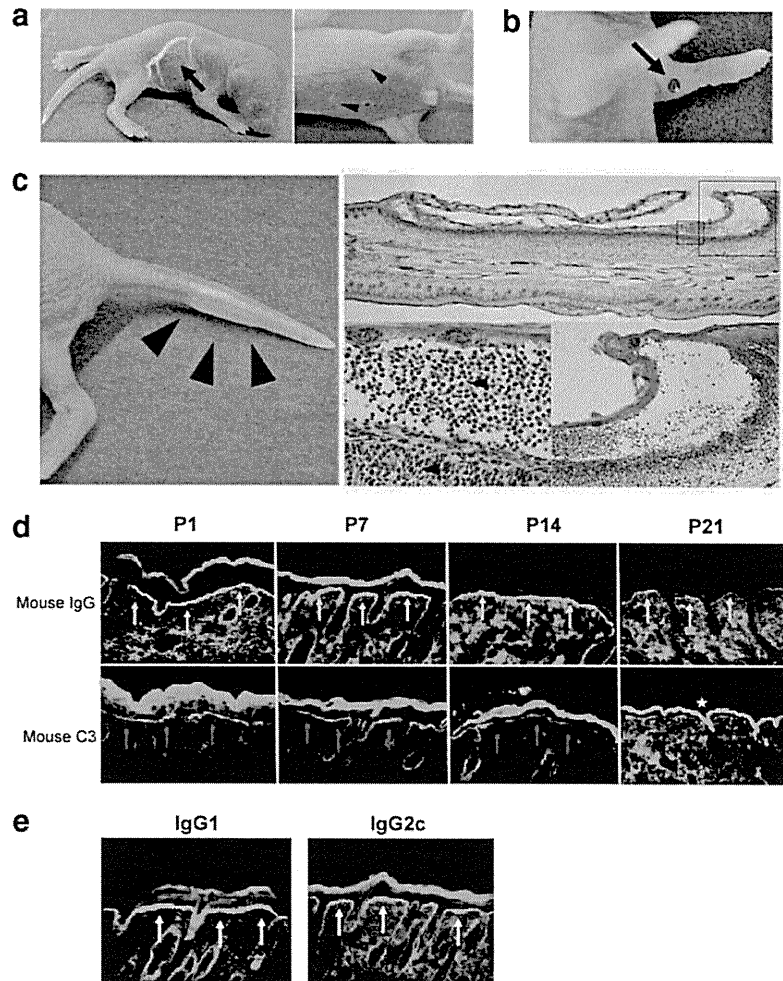
FIGURE 3. *a*, Neonatal BP mice showed severe skin fragility, with the epidermis easily detaching from mechanical friction (Nikolsky phenomenon, arrow). Spontaneous small blisters and pustules were scattered over the entire body (arrowheads). *b*, Small, round, crusted lesion developed around the arm in 4-day-old neonatal BP mice. *c*, Histological finding of blistering lesion on the tail. Subepidermal blister formation associated with numerous infiltrations of neutrophils (arrowheads) was observed. *d*, DIF study revealed in vivo skin deposition of mouse IgG (yellow arrows) until 3 wk after birth, and activated mouse C3 (red arrows) was detected within 1 to 2 wk after birth. Note the Abs to mouse C3 strongly cross-reacted to the corneal layer of the epidemis (star). *e*, In vivo deposition of IgG1 and IgG2c was detected at the dermal-epidermal junction of a neonatal BP mouse soon after birth (arrows).

Maternal IgG to human COL17 was transmissible into neonatal circulation via milk even after birth

Interestingly, some of the mice showed elevated IgG Ab titers to human COL17 by ELISA around 1 to 2 wk after birth (Fig. 2*d*). It
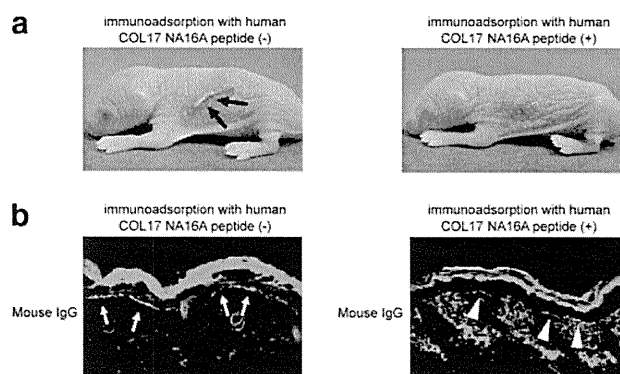

FIGURE 4. IgG Abs to the NC16A domain of human COL17 play a major role in inducing blistering skin disease. *a*, Neonatal COL17-humanized (*mColl7$^{-/-}$, hCOL17$^{+/+}$*) mice that received IgG Abs without immunoadsorption with human COL17 NC16A protein from immunized *mColl7$^{+/-}$* females resulted in skin fragility (positive Nikolsky sign, arrows), whereas no epidermal detachment could be observed in mice that received immune-adsorbed IgG (50 μl of 2.1 μg/μl IgG Abs, respectively). *b*, In vivo deposition of mouse IgG was more intense in the skin obtained from mice that received IgG Abs without adsorption with human COL17 NC16A protein (arrows) compared with that being adsorbed with the protein (arrowheads).

has been reported that mouse IgG can be transferred from milk via neonatal FcR expressed in gut, which is different from humans (2, 21, 22). To investigate this possibility, COL17-humanized (*mColl7$^{-/-}$, hCOL17$^{+/+}$*) neonatal mice delivered from unrelated pairs were moved soon after birth to a lactating preimmunized *mColl7$^{+/-}$* female mouse (ELISA index value to human COL17 of 1.33). As a result, it was found that, at 1 wk of breast-feeding from the immunized female mouse, serum IgG in these pups to human COL17 was markedly elevated (ELISA index titer: 0.73 ± 0.20, *n* = 4), and mouse IgG reacted positively to the dermal-epidermal junction in the skin until 1/1280 dilution (Fig. 5*a*). In contrast, IgG Abs to human COL17 of the pups breast-fed from the nonimmunized female mouse were not increased (ELISA index titer: 0.02 ± 0.03, *n* = 4), and mouse IgG did not react to the normal human skin (Fig. 5*a*). These results clearly indicate that maternally anti-human COL17 IgG Abs were transmitted from milk. However, these COL17-humanized (*mColl7$^{-/-}$, hCOL17$^{+/+}$*) neonatal mice with maternal milk-derived Abs to human COL17 in their circulation showed no skin fragility (data not shown). In Neonatal BP mice, active blistering skin disease could be observed for several days after birth, therefore, we assessed in vivo deposition of mouse IgG in the neonatal COL17-humanized (*mColl7$^{-/-}$, hCOL17$^{+/+}$*) mice skin at 2 days after being breast-fed by the lactating preimmunized *mColl7$^{+/-}$* female to find how maternal IgG from milk could contribute to the blistering skin disease soon after birth. As a result, very low amount of mouse IgG could be detected at the dermal-epidermal junction
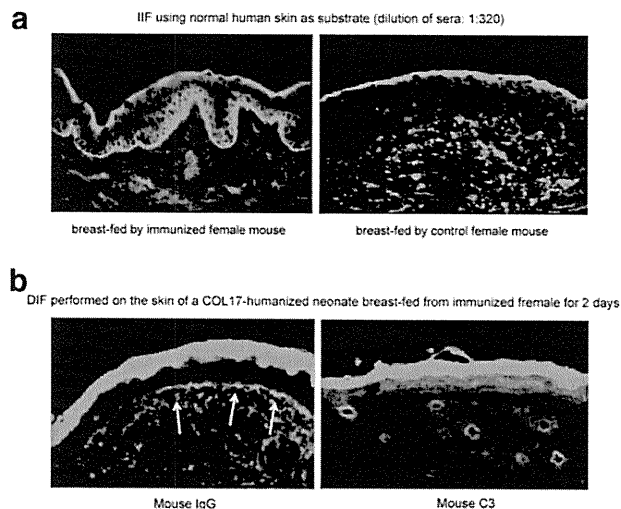
a   IIF using normal human skin as substrate (dilution of sera: 1:320)

breast-fed by immunized female mouse   breast-fed by control female mouse

b   DIF performed on the skin of a COL17-humanized neonate breast-fed from immunized fremale for 2 days

Mouse IgG   Mouse C3

FIGURE 5. Maternal anti-human COL17 Abs transferred from milk. a, Serum IgG in these pups to human COL17 reacted to the dermal-epidermal junction at 1 wk of breast-feeding from an immunized female mouse (1/320 dilution). b, COL17-humanized ($mCol17^{-/-}$, $hCOL17^{+/+}$) neonatal mice skin at 2 days of breast-feeding from an immunized mother mouse showed mild in vivo deposition of IgG Abs along the dermal-epidermal junction.

(Fig. 5b), suggesting that IgG from milk would play a minor role in the pathogenesis of this Neonatal BP mice model.

Discussion

This study showed successful production of a novel autoimmune disease model in which efficiently transferred maternal IgG induced distinctive Ab-mediated blistering skin disease in COL17-humanized neonates. The COL17 is crucial for maintaining the structural stability of skin. Indeed, loss of COL17 in skin as a result of null mutations results in a novel form of epidermolysis bullosa (OMIM: 226650) (23, 24). Similarly, $mCol17^{-/-}$ mice skin is so fragile that these mice could not be intercrossed (12). Therefore, we used heterozygote-null, but phenotypically normal $mCol17^{+/-}$ female mice to develop Abs against human COL17. Furthermore, by mating immunized female mice with COL17-humanized male mice, human COL17 could be introduced into neonates as an Ag. This simple method enabled us to develop distinctive neonatal BP mice that demonstrate a more severe blistering phenotype characterized by spontaneous blister formation with numerous inflammatory cell infiltrates, a phenotype that is very similar to that seen in humans with BP (15, 16).

Our neonatal BP mice has several advantages over previous mouse models of BP (12, 14). First, unlike other BP models that have relied on the injection of pathogenic IgG Abs into neonatal mice, our model does not require the technically difficult injection procedure. Second, the pathogenic IgG remains in circulation longer in the new model than in conventional models that use injected IgG. Third, the immune reaction is totally dependent on the mouse immune system, while the Ag remains human COL17. The mouse complement system does not work as efficiently during the neonatal period as during adulthood (25). Accordingly, the present system using Abs from the same species is suitable for promoting the subsequent inflammation cascade, including activation of the mouse complement. Finally, immunized heterozygous $mCol17^{+/-}$ female mice induced both IgG1 and IgG2c autoAbs which were transferred to neonates. Mouse IgG1 Abs do not fix complement (20), whereas IgG2c does fix mouse complement (26); therefore, activation of com-

plement in the present system would be induced predominately by IgG2c. Activation of complement has been reported to play a pivotal role in BP blistering (27, 28). In light of this, the current model can be regarded as accurately reproducing human BP disease.

Maternal IgG Abs to human COL17, especially to the NC16A domain, via placenta plays a major role in the current neonatal BP mice model to induce blistering skin disease, in which the most severe disease could be observed soon after birth. However, although it is a rare possibility, maternal transferred lymphocytes as well as pathogenic IgG from milk might contribute to the blistering skin disease. In particular, we were able to clearly demonstrate that maternal IgG Abs transferred into pups via milk 1 wk after birth, although no active blistering skin disease could be observed in the recipient unrelated COL17-humanized ($mCol17^{-/-}$, $hCOL17^{+/+}$) neonatal mice. The reason we could not observe blistering skin disease is probably due to the lower amount of IgG to human COL17 than in neonatal BP mice, in which maternal IgG could be transferred from not only milk but also via placenta, especially soon after birth. IgG transferred from milk might work in part, but it will not be a major player in inducing blistering skin disease, because blistering skin disease was the most severe soon after birth and no active blistering skin disease could be observed at 1 wk, when a lot of fur had grown.

Using maternally transferred pathogenic Abs and introducing human Ags in neonates, we succeeded in inducing autoimmune disease model in neonates whose Ags are functionally important. However, this system does not truly represent autoimmunity in human patients, because Abs to human COL17 in diseased neonates are transferred Abs. In addition, for immunized heterozygote $Col17$-deficient ($mCol17^{+/-}$) female mice, human COL17 is not an autoAg but alloantigen therefore, pathogenic Abs to human COL17 in this system is not strictly an autoAbs. Nevertheless, maternally transferred Abs in genetically transformed Ag-humanized neonates will be useful in the study of autoimmune diseases as a novel method for generating diseases in neonates.

Disclosures

The authors have no financial conflict of interest.

References

1. Kohler, P. F., and R. S. Farr. 1966. Elevation of cord over maternal IgG immunoglobulin: evidence for an active placental IgG transport. *Nature* 210: 1070–1071.
2. Van de Perre, P. 2003. Transfer of antibody via mother's milk. *Vaccine* 21: 3374–3376.
3. Lee, L. A. 1993. Neonatal lupus erythematosus. *J. Invest. Dermatol.* 100: 9S–13S.
4. Lee, L. A., M. B. Frank, V. R. McCubbin, and M. Reichlin. 1994. Autoantibodies of neonatal lupus erythematosus. *J. Invest. Dermatol.* 102: 963–966.
5. Vernet-der Garabedian, B., M. Lacokova, B. Eymard, E. Morel, M. Feltin, J. Zajac, O. Sadovsky, M. Dommergues, and J. F. Bach. 1994. Association of neonatal myasthenia gravis with antibodies against the fetal acetylcholine receptor. *J. Clin. Invest.* 94: 555–559.
6. Ni, H., P. Chen, C. M. Spring, E. Sayeh, J. W. Semple, A. H. Lazarus, R. O. Hynes, and J. Freedman. 2006. A novel murine model of fetal and neonatal alloimmune thrombocytopenia: response to intravenous IgG therapy. *Blood* 107: 2976–2983.
7. van der Neut, R., P. Krimpenfort, J. Calafat, C. M. Niessen, and A. Sonnenberg. 1996. Epithelial detachment due to absence of hemidesmosomes in integrin β 4 null mice. *Nat. Genet.* 13: 366–369.
8. Georges-Labouesse, E., N. Messaddeq, G. Yehia, L. Cadalbert, A. Dierich, and M. Le Meur. 1996. Absence of integrin α 6 leads to epidermolysis bullosa and neonatal death in mice. *Nat. Genet.* 13: 370–373.
9. Ryan, M. C., K. Lee, Y. Miyashita, and W. G. Carter. 1999. Targeted disruption of the LAMA3 gene in mice reveals abnormalities in survival and late stage differentiation of epithelial cells. *J. Cell Biol.* 145: 1309–1323.

10. Heinonen, S., M. Männikkö, J. F. Klement, D. Whitaker-Menezes, G. F. Murphy, and J. Uitto. 1999. Targeted inactivation of the type VII collagen gene (Col7a1) in mice results in severe blistering phenotype: a model for recessive dystrophic epidermolysis bullosa. *J. Cell. Sci.* 112: 3641–3648.

11. Meng, X., J. F. Klement, D. A. Leperi, D. E. Birk, T. Sasaki, R. Timpl, J. Uitto, and L. Pulkkinen. 2003. Targeted inactivation of murine laminin γ2-chain gene recapitulates human junctional epidermolysis bullosa. *J. Invest. Dermatol.* 121: 720–731.

12. Nishie, W., D. Sawamura, M. Goto, K. Ito, A. Shibaki, J. R. McMillan, K. Sakai, H. Nakamura, E. Olasz, K. B. Yancey, et al. 2007. Humanization of autoantigen. *Nat. Med.* 14: 378–383.

13. Anhalt, G. J., C. F. Bahn, R. S. Labib, J. J. Voorhees, A. Sugar, and L. A. Diaz. 1981. Pathogenic effects of bullous pemphigoid autoantibodies on rabbit corneal epithelium. *J. Clin. Invest.* 68: 1097–1101.

14. Liu, Z., L. A. Diaz, J. L. Troy, A. F. Taylor, D. J. Emery, J. A. Fairley, and G. J. Giudice. 1993. A passive transfer model of the organ-specific autoimmune disease, bullous pemphigoid, using antibodies generated against the hemidesmosomal antigen. BP180. *J. Clin. Invest.* 92: 2480–2488.

15. Korman, N. 1987. Bullous pemphigoid. *J. Am. Acad. Dermatol.* 16: 907–924.

16. Stanley, J. R., P. Hawley-Nelson, S. H. Yuspa, E. M. Shevach, and S. I. Katz. 1982. Characterization of bullous pemphigoid antigen: a unique basement membrane protein of stratified squamous epithelia. *Cell* 24: 897–903.

17. Gatalica, B., L. Pulkkinen, K. Li, K. Kuokkanen, M. Ryynänen, J. A. McGrath, and J. Uitto. 1997. Cloning of the human type XVII collagen gene (COL17A1), and detection of novel mutations in generalized atrophic benign epidermolysis bullosa. *Am. J. Hum. Genet.* 60: 352–365.

18. Zillikens, D., P. A. Rose, S. D. Balding, Z. Liu, M. Olague-Marchan, L. A. Diaz, and G. J. Giudice. 1997. Tight clustering of extracellular BP180 epitopes recognized by bullous pemphigoid autoantibodies. *J. Invest. Dermatol.* 109: 573–579.

19. Olasz, E. B., J. Roh, C. L. Yee, K. Arita, M. Akiyama, H. Shimizu, J. C. Vogel, and K. B. Yancey. 2007. Human bullous pemphigoid antigen 2 transgenic skin elicits specific IgG in wild-type mice. *J. Invest. Dermatol.* 127: 2807–2817.

20. Sitaru, C., M. T. Chiriac, S. Mihai, J. Büning, A. Gebert, A. Ishiko, and D. Zillikens. 2006. Induction of complement-fixing autoantibodies against type VII collagen results in subepidermal blistering in mice. *J. Immunol.* 177: 3461–3468.

21. Appleby, P., and D. Catty. 1983. Transmission of immunoglobulin to foetal and neonatal mice. *J. Reprod. Immunol.* 5: 203–213.

22. Israel, E. J., V. K. Patel, S. F. Taylor, A. Marshak-Rothstein, and N. E. Simister. 1995. Requirement for a β_2-microglobulin-associated Fc receptor for acquisition of maternal IgG by fetal and neonatal mice. *J. Immunol.* 154: 6246–6251.

23. McGrath, J. A., B. Gatalica, A. M. Christiano, K. Li, K. Owaribe, J. R. McMillan, R. A. Eady, and J. Uitto. 1995. Mutations in the 180-kD bullous pemphigoid antigen (BPAG2), a hemidesmosomal transmembrane collagen (COL17A1), in generalized atrophic benign epidermolysis bullosa. *Nat. Genet.* 11: 83–86.

24. Shimizu, H., Y. Takizawa, L. Pulkkinen, J. J. Zone, K. Matsumoto, T. Saida, J. Uitto, and T. Nishikawa. 1998. The 97 kDa linear IgA bullous dermatosis antigen is not expressed in a patient with generalized atrophic benign epidermolysis bullosa with a novel homozygous G258X mutation in COL17A1. *J. Invest. Dermatol.* 111: 887–892.

25. Pihlgren, M., A. Fulurija, M. B. Villiers, C. Tougne, P. H. Lambert, C. L. Villiers, and C. A. Siegrist. 2004. Influence of complement C3 amount on IgG responses in early life: immunization with C3b-conjugated antigen increases murine neonatal antibody responses. *Vaccine.* 23: 329–335.

26. Baudino, L., S. Azeredo da Silveria, M. Nakata, and S. Izui. 2006. Molecular and cellular basis for pathogenicity of autoantibodies: lessons from murine monoclonal autoantibodies. *Springer. Semin. Immunopathol.* 28: 175–184.

27. Liu, Z., G. J. Giudice, S. J. Swartz, J. A. Fairley, G. O. Till, J. L. Troy, and L. A. Diaz. 1995. The role of complement in experimental bullous pemphigoid. *J. Clin. Invest.* 95: 1539–1544.

28. Nelson, K. C., M. Zhao, P. R. Schroeder, N. Li, R. A. Wetsel, L. A. Diaz, and Z. Liu. 2006. Role of different pathways of the complement cascade in experimental bullous pemphigoid. *J. Clin. Invest.* 116: 2892–2900.

Novel mutation p.Gly59Arg in *GJB6* encoding connexin 30 underlies palmoplantar keratoderma with pseudoainhum, knuckle pads and hearing loss

I. Nemoto-Hasebe, M. Akiyama, S. Kudo,* A. Ishiko,* A. Tanaka,† K. Arita and H. Shimizu

Department of Dermatology, Hokkaido University Graduate School of Medicine, North 15 West 7, Sapporo 060-8638, Japan
*Department of Dermatology, Keio University School of Medicine, Tokyo, Japan
†Department of Dermatology, Kameda General Hospital, Chiba, Japan

Summary

Background Connexins, components of the gap junction, are expressed in several organs including the skin and the cochlea. Mutations in connexin genes including GJB2 (Cx26), GJB3 (Cx31), GJB4 (Cx30.3), GJB6 (Cx30) and GJA1 (Cx43) are responsible for various dermatological syndromes and/or inherited hearing loss, frequently showing overlapping phenotypes.
Objectives To clarify the spectrum of clinical phenotypes caused by connexin mutations.
Methods We report a 32-year-old Japanese woman with mild palmoplantar keratoderma (PPK) with severe sensorineural hearing loss, knuckle pads and pseudoainhum of her toes.
Results Direct sequencing revealed no mutation in GJB2, but a novel heterozygous missense mutation p.Gly59Arg in GJB6. Electron microscopy revealed no apparent morphological abnormality of gap junctions in the patient's lesional epidermis.
Conclusions The patient harboured the novel GJB6 missense mutation p.Gly59Arg in the first extracellular loop of Cx30. Mutations in glycine 59 of Cx26 are associated with PPK–deafness syndrome, and the similar phenotype here supports the observed heteromeric channel formation; the dominant nature of the mutation suggests an effect on gap junctions similar to that of the comparable mutation in Cx26.

Gap junctions are cell-to-cell connecting structures containing clusters of intercellular channels that allow intercellular passage of ions and molecules of up to 1 kDa. These channels are oligomeric assemblies of family members of related proteins called connexins. Six connexin polypeptides assemble into a connexon, a hemichannel that interacts with its counterpart in an adjacent cell membrane to form a complete intercellular channel.[1] All the connexins in an individual connexon may be of the same type (homomeric), or heteromeric connexons may be formed by oligomerization between different connexins. Connexin 26 (Cx26) and connexin 30 (Cx30) are known to form heteromeric connexon hemichannels.[2]

Connexins are expressed in several organs including the skin and the cochlea. Mutations in connexin genes including GJB2 (Cx26), GJB3 (Cx31), GJB4 (Cx30.3), GJB6 (Cx30) and GJA1 (Cx43) are responsible for several hereditary skin disorders associated with hearing loss.[3] Cx30 mutations are typically associated with Clouston syndrome[4] in which palmoplantar keratoderma (PPK) is only occasional and not usual, although cases resembling keratitis–ichthyosis–deafness (KID) syndrome have also been reported.[5] Various mutations affecting Cx26 cause PPK–deafness syndrome.[6] PPK–deafness syndromes are typically GJB2 associated. However, as Cx26 and Cx30 interact, one might expect more phenotypic overlap as exemplified by the report of Jan et al.[5]

Here, we report a Japanese woman with clinical features resembling those of Vohwinkel syndrome and Bart–Pumphrey syndrome. We found a novel heterozygous missense mutation p.Gly59Arg in GJB6. As far as we know, this is the first reported patient with PPK with pseudoainhum, knuckle pads and hearing loss, harbouring a GJB6 gene mutation.

Patients and methods

Patient

The patient was a 32-year-old Japanese woman. She was diagnosed with congenital sensorineural hearing loss when she
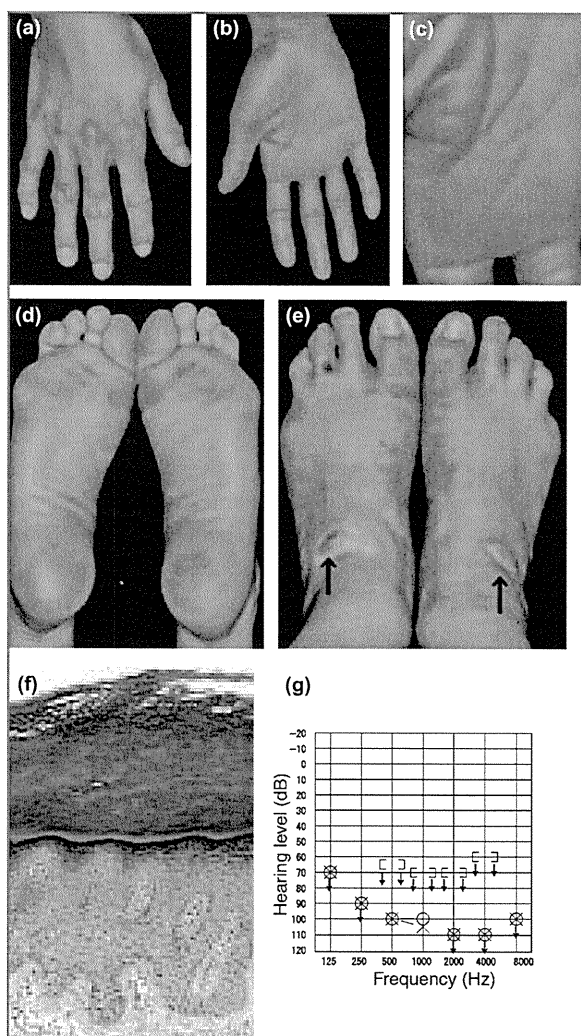
Fig 1. (a–e) Clinical features of the patient's skin. (a) Knuckle pads on the dorsa of the fingers of the patient; (b–d) diffuse palmar and plantar hyperkeratosis without honeycomb features; (d, e) amputation due to constriction bands on the fifth toe of each foot; extensive hyperkeratosis was seen on the ankle joints. (f) Skin biopsy from the sole revealed marked orthohyperkeratosis with hypergranulosis (haematoxylin and eosin; original magnification × 100). (g) Patient's pure tone audiogram showed pronounced sensory hearing loss: air conduction indicated by cross/round marks (cross, left ear; round, right ear); bone conduction indicated by bracket marks ([, right ear;], left ear); arrows pointing downwards indicate the loudest tone that was not heard.

was 3 years old. She also had diffuse PPK without a honeycomb hyperkeratosis appearance and hyperkeratotic plaques over the knuckles (Fig. 1a–c). An audiogram obtained at 24 years of age showed pronounced sensorineural hearing loss (Fig. 1g). At the age of 26 years, the fifth toe on each foot was surgically amputated due to pseudoainhum (Fig. 1d,e). Her fingers did not show mutilation. Extensive hyperkeratosis was seen in areas exposed to mechanical stress, such as the extensor (ventral) aspect of her ankle joints (Fig. 1e) probably because of folding the legs in the Japanese sitting or kneeling

style. She had no features of ichthyosis on her trunk or extremities. Her hair, teeth and nails were normal and she had no ocular involvement. There was no family history of skin disorders or auditory dysfunction, or consanguinity in her family. All members of the family, including her parents and her elder sister, were generally healthy and were without PPK or hearing loss.

Mutation detection

After fully informed, written consent, peripheral blood samples were obtained from the patient and genomic DNA was extracted (Qiagen, Hilden, Germany). The entire coding region and exon/intron boundaries of *GJB2* and *GJB6* were amplified by polymerase chain reaction (PCR) using the specific primers described previously.[7,8] PCR products were sequenced and mutation was confirmed by enzyme digestion with BtgZI restriction enzymes (New England Biolabs, Ipswich, MA, U.S.A.). Reference cDNA for *GJB6* was cDNA sequence GenBank accession number NT_009799.

Morphological observations

A skin biopsy was taken from the right sole of the patient with fully informed consent. The biopsy specimen was processed for routine histological analysis and for ultrastructural observations as previously described.[9]

Results

Mutation analysis

Analysis in *GJB2* revealed no mutation, although a common polymorphism p.Val27Ile was found. We identified a heterozygous 175G>C transversion in *GJB6* (Fig. 2a). This novel nucleotide alteration leads to the replacement of glycine 59 (neutral, hydrophilic residue) with a positively charged hydrophilic arginine residue (p.Gly59Arg) in the first extracellular loop. The mutation introduces a single BtgZI restriction site in the gene. We confirmed the presence of the mutation in the patient's genomic DNA by restriction enzyme BtgZI digestion (Fig. 2b). This nucleotide change was not detected in 100 unrelated, healthy Japanese individuals (200 alleles).

Histological evaluation of the patient's skin

A biopsy specimen from the patient's plantar skin revealed compact orthohyperkeratosis with hypergranulosis and acanthosis in the epidermis (Fig. 1f).

Electron microscopic findings

Ultrastructurally, keratinocytes in the epidermis of the patient's plantar skin assembled gap junctions showing normal morphology with a typical pentalaminar structure, 20 nm in width (data not shown).
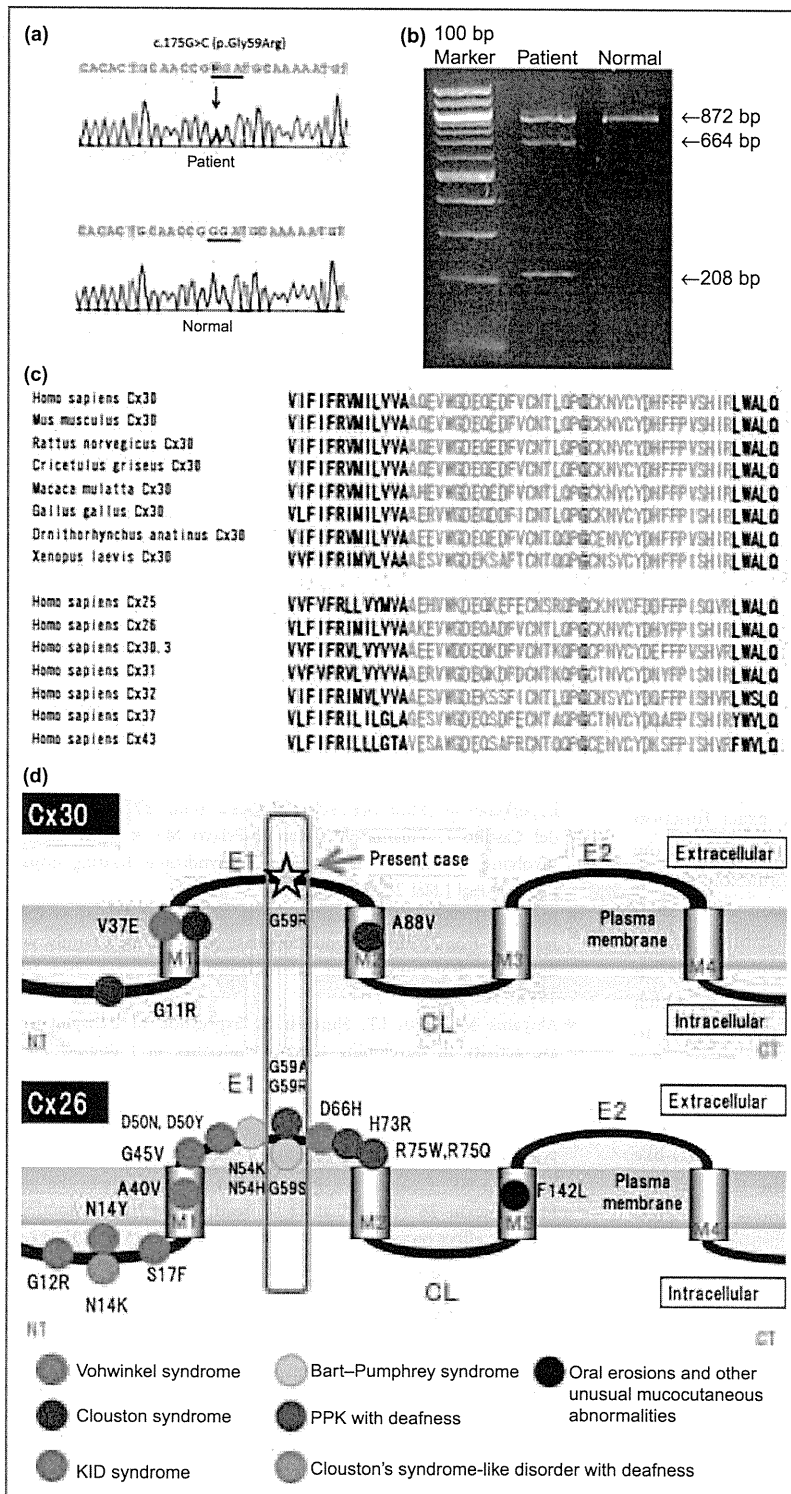
Fig 2. (a) Sequence chromatograms of *GJB6* from the patient (upper) showed the heterozygous transition c.175G>C at codon 59 (p.Gly59Arg). (b) Confirmation of the presence of the mutation p.Gly59Arg in the patient by *Btg*ZI restriction digestion. An 872 bp polymerase chain reaction fragment from the mutant allele was digested into 664 bp and 208 bp fragments, whereas that from the wild-type allele was not cut. Thus, 872 bp, 664 bp and 208 bp bands were seen in the patient harbouring the heterozygous p.Gly59Arg mutation, although only a 872 bp band was detected in the normal control. (c) Comparison of amino acid sequences of Cx30 from diverse species and other members of the human connexin family. Glycine residue at codon position 59 (red) is located in the centre of the first extracellular domain (blue) and is highly conserved in diverse species and other members of the human connexin family. (d) Cx30/Cx26-associated syndromes and reported causative mutations in Cx30/Cx26. M1–M4, transmembrane domains 1–4, respectively; E1 and E2, extracellular domains 1 and 2, respectively; CL, cytoplasmic loop; PPK, palmoplantar keratoderma; KID, keratitis–ichthyosis–deafness.

Discussion

We herewith report, as far as we know, the first case of PPK–deafness caused by a mutation affecting the E1 domain of Cx30. Glycine 59 in Cx30 is located in the first extracellular loop (Fig. 2c,d), which exhibits high sequence conservation in homologous proteins from different species (Fig. 2c). The first extracellular loop is thought to be essential for the

interaction between a connexon and its counterpart in an adjacent cell to form a complete intercellular channel. Three mutations in Cx26, p.Gly59Ala, p.Gly59Trp and p.Gly59Ser, occur at glycine 59 which is orthologous to glycine 59 in Cx30. These were reported in syndromes comprising sensorineural hearing loss and PPK[6,10] (Fig. 2d).

Cx30 and Cx26 form heteromeric junctions both in the skin and the inner ear and functional data suggest a dominant interaction between the two.[2,11] From these facts, we think it reasonable to speculate that missense mutations in the first extracellular loop domain in either Cx26 or Cx30 can lead to similar phenotypes. However, this hypothesis does not explain why the phenotypes look so similar or why, for example, p.Gly11Arg in Cx30 does not lead to KID syndrome whereas p.Gly12Arg in Cx26 does. There may be a genetic background effect which contributes to the phenotype in each patient.

The GJB2 keratoderma/deafness phenotypes are almost all caused by mutations clustering in the first extracellular loop domain.[12] The Cx26 mutation p.Gly59Arg results in a diffuse (although more severe) keratoderma, as does this mutation in Cx30 which is shown in the present patient. In contrast, mutations in the N-terminal cytoplasmic region in Cx26 are associated with KID syndrome and similar phenotypes. Likewise, p.Gly11Arg and p.Val37Glu in Cx30 in the N-terminal cytoplasmic region underlie KID-like syndrome or Clouston syndrome. We do not know the exact function of the N-terminal domain. There are two hypotheses: the first is that the N-terminus is involved in connexon assembly;[13] the second is that the N-terminal domain works as a plug in a vestibule of the connexon hemichannel, which physically blocks the channel (plug gating mechanism).[14] It was suggested that the mutation p.Asn14Tyr in Cx26, which is associated with a KID phenotype, causes the channel to be locked in a closed position by the plug.[15] Thus, if a similar phenomenon happens with the Cx30 mutation in a heteromeric channel composed of Cx30 and Cx26, Cx30 mutations in the N-terminus may lead to similar KID-like phenotypes. The present patient harbouring the Cx30 mutation in the first extracellular loop domain showed a phenotype distinct from KID syndrome.

Light microscopic observation of the lesional skin showed orthohyperkeratosis with hypergranulosis without any specific findings for our present patient. The mutation we found did not affect connexin morphology. Likewise, some Cx26 mutations in the E1 domain were examined for their effects on connexin morphology and apparently did not affect it.[11,16]

In conclusion, we present a novel GJB6 missense mutation p.Gly59Arg in a patient who had PPK with pseudoainhum, knuckle pads and hearing loss. The present case expands the clinical spectrum of GJB6 mutations and shows that, in PPK–deafness cases where we do not find GJB2 mutations, we should check GJB6. Furthermore, our results suggest an interaction between Cx30 and Cx26 E1 domains.

References

1 Yeager M, Nicholson BJ. Structure of gap junction intercellular channels. *Curr Opin Struct Biol* 1996; **6**:183–92.

2 Forge A, Marziano NK, Casalotti SO *et al.* The inner ear contains heteromeric channels composed of cx26 and cx30 and deafness-related mutations in cx26 have a dominant negative effect on cx30. *Cell Commun Adhes* 2003; **10**:341–6.

3 Grifa A, Wagner CA, D'Ambrosio L *et al.* Mutations in GJB6 cause nonsyndromic autosomal dominant deafness at DFNA3 locus. *Nat Genet* 1999; **23**:16–18.

4 Lamartine J, Munhoz Essenfelder G, Kibar Z *et al.* Mutations in GJB6 cause hidrotic ectodermal dysplasia. *Nat Genet* 2000; **26**:142–4.

5 Jan AY, Amin S, Ratajczak P *et al.* Genetic heterogeneity of KID syndrome: identification of a Cx30 gene (GJB6) mutation in a patient with KID syndrome and congenital atrichia. *J Invest Dermatol* 2004; **122**:1108–13.

6 Heathcote K, Syrris P, Carter ND *et al.* A connexin 26 mutation causes a syndrome of sensorineural hearing loss and palmoplantar hyperkeratosis (MIM 148350). *J Med Genet* 2000; **37**:50–1.

7 del Castillo I, Villamar M, Moreno-Pelayo MA *et al.* A deletion involving the connexin 30 gene in nonsyndromic hearing impairment. *N Engl J Med* 2002; **346**:243–9.

8 Richard G, White TW, Smith LE *et al.* Functional defects of Cx26 resulting from a heterozygous missense mutation in a family with dominant deaf-mutism and palmoplantar keratoderma. *Hum Genet* 1998; **103**:393–9.

9 Akiyama M, Smith LT, Shimizu H. Expression of transglutaminase activity in developing human epidermis. *Br J Dermatol* 2000; **142**:223–5.

10 Alexandrino F, Sartorato EL, Marques-de-Faria AP *et al.* G59S mutation in the GJB2 (connexin 26) gene in a patient with Bart–Pumphrey syndrome. *Am J Med Genet A* 2005; **136**:282–4.

11 Marziano NK, Casalotti SO, Portelli AE *et al.* Mutations in the gene for connexin 26 (GJB2) that cause hearing loss have a dominant negative effect on connexin 30. *Hum Mol Genet* 2003; **12**:805–12.

12 de Zwart-Storm EA, Hamm H, Stoevesandt J *et al.* A novel missense mutation in GJB2 disturbs gap junction protein transport and causes focal palmoplantar keratoderma with deafness. *J Med Genet* 2008; **45**:161–6.

13 Kyle JW, Minogue PJ, Thomas BC *et al.* An intact connexin N-terminus is required for function but not gap junction formation. *J Cell Sci* 2008; **121**:2744–50.

14 Oshima A, Tani K, Hiroaki Y *et al.* Three-dimensional structure of a human connexin26 gap junction channel reveals a plug in the vestibule. *Proc Natl Acad Sci USA* 2007; **104**:10034–9.

15 Arita K, Akiyama M, Aizawa T *et al.* A novel N14Y mutation in connexin26 in keratitis–ichthyosis–deafness syndrome. *Am J Pathol* 2006; **169**:416–23.

16 Essenfelder GM, Bruzzone R, Lamartine J *et al.* Connexin30 mutations responsible for hidrotic ectodermal dysplasia cause abnormal hemichannel activity. *Hum Mol Genet* 2004; **13**:1703–14.

Spontaneous Giant Aneurysm of the
Superficial Temporal Artery

—Case Report—

Masahito KAWABORI, Satoshi KURODA, Naoki NAKAYAMA, Yasuko KENMOTSU*,
Hiroshi SHIMIZU*, Michie TANINO**, and Yoshinobu IWASAKI

*Departments of Neurosurgery, *Dermatology, and **Pathology,
Hokkaido University Graduate School of Medicine, Sapporo, Hokkaido*

Abstract

A 78-year-old woman presented with preauricular superficial temporal artery (STA) aneurysm and scalp porocarcinoma, which had both increased in size over 2 years. She had no previous history of head trauma. Three-dimensional (3D) computed tomography (CT) angiography revealed a 4-cm diameter STA aneurysm arising from the main trunk of the left STA and located just lateral to the zygomatic arch. The scalp porocarcinoma was excised by dermatologists. The STA aneurysm was carefully dissected from the surrounding tissues, and was resected after ligation of the proximal STA. Histological examination showed the aneurysm consisted of intima, media, and adventitia, and the diagnosis was atherosclerotic fusiform aneurysm. 3D CT angiography is quite useful to plan surgical strategy for such an unusually large STA aneurysm.

Key words: superficial temporal artery, true aneurysm, giant aneurysm, three-dimensional computed tomography angiography

Introduction

Traumatic aneurysm of the superficial temporal artery (STA) is not unusual, with more than 400 reported cases,[13] including the first case in 1740.[4] Traumatic STA aneurysm usually develops in young adult men at 2 to 6 weeks after blunt head trauma,[11] and the majority are pseudoaneurysms. Spontaneous or non-traumatic STA aneurysms are quite rare, with only 16 cases described.[1,2,4,5,7,9,10,12,15] Histological examination confirmed "true" aneurysm in 7 of these cases,[1,2,5,7,9,10,12] and 3 were giant true STA aneurysm, with more than 25-mm diameter.[1,2,5]

Here we describe a case of giant true STA aneurysm of 47-mm diameter that gradually increased in size over 2 years.

Case Report

A 78-year-old female first noticed two masses in the left temporal region 2 years previously, but did not consult a physician because of the absence of pain or discomfort. However, both masses gradually increased in size over 2 years, so she visited our hospital. She had no history of head trauma. Physical examination found a painless, pulsatile mass in the left preauricular area, and a black, hairy non-pulsatile mass in the left temporal region (Fig. 1). First, she was admitted to the Department of Dermatology and underwent surgical resection of the non-pulsatile mass. The histological diagnosis was porocarcinoma. She was then admitted to our department.

The pulsatile mass was round and about 4 cm in diameter. The left external auditory meatus was almost obstructed by the mass. Facial nerve function was intact. Computed tomography (CT) with contrast medium demonstrated homogeneous enhancement. Three-dimensional (3D) CT angiography revealed that the aneurysm arose from the main trunk of the left STA, which was located medial to the mass. The distal STA was not visible, probably because the blood flow was delayed due to turbulent flow in the huge aneurysm (Fig. 2). Magnetic resonance (MR) imaging and ultrasonography showed turbulent flow within the aneurysm. Based on these physical and radiological findings, our diagnosis was a non-traumatic, giant STA aneurysm.
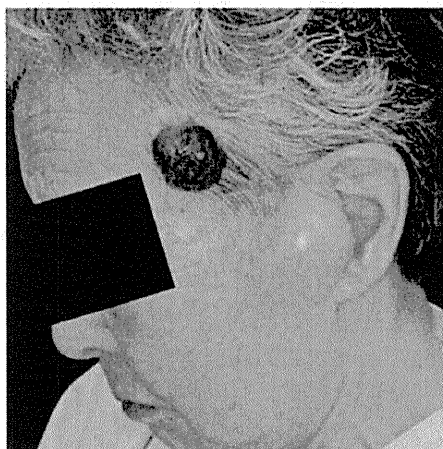
198

Fig. 1　Photograph showing a huge pulsating tumor
in the left preauricular region (4 × 4 × 4
cm) and a hairy, black tumor in the left tem-
poral region (3 × 3 × 2 cm).

Fig. 2　Three-dimensional computed tomography
angiograms demonstrating a giant
aneurysm arising from the main trunk of
left superficial temporal artery (STA), and
located lateral to the zygomatic arch (A),
and the proximal STA located medial to the
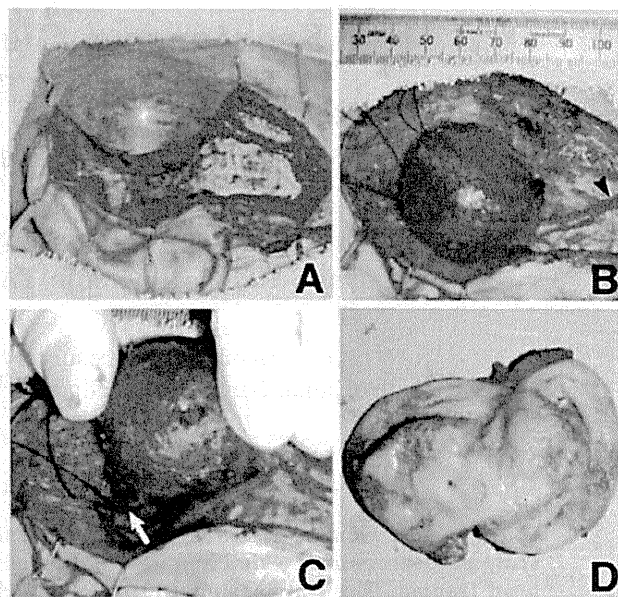aneurysm (B, *arrow*).

Fig. 3　Intraoperative photographs showing the
parietal branch of the superficial temporal
artery (STA) and the aneurysm covered by
the skin (A). The aneurysm and the parietal
branch of the STA (*arrowhead*), seen at the
distal end of aneurysm, were completely ex-
posed (B). The proximal STA medial to the
aneurysm was dissected and ligated (C, *ar-
row*). The resected aneurysm had thickened
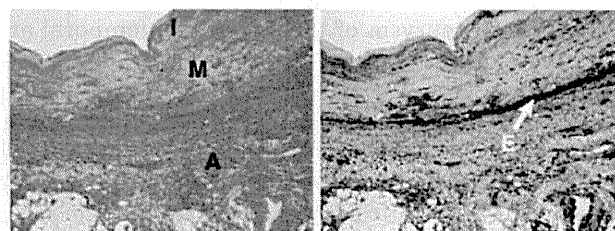wall around the orifice (D).

Fig. 4　Photomicrographs of the resected aneurysm
showing preservation of the intima (I), me-
dia (M), and adventitia (A), and fragmenta-
tion of the elastic membrane (E, *arrow*).
Hematoxylin and eosin stain (*left*) and
elastica Masson stain (*right*), original mag-
nification × 200.

She underwent surgical excision under general
anesthesia. After exposure of the distal STA, the
aneurysm was carefully dissected from the sur-
rounding tissues, including the temporal fascia,
parotid gland, and zygomatic arch. The dissected
aneurysm was rotated and the proximal STA was li-
gated. Finally, the aneurysm was resected (Fig. 3).
The aneurysm was 47 mm × 45 mm × 35 mm with
thickened wall. Histological examination revealed
that the aneurysm consisted of the intima, media,
and adventitia, and the elastic membrane was ex-
tended and fragmented. No malignant or inflamma-
tory cells were found in the specimen. The histologi-
cal diagnosis was a true aneurysm (Fig. 4). She was

discharged without neurological deficits.

Discussion

Eight cases of histologically verified, spontaneous
true STA aneurysm have been reported, including

Table 1 Previous cases of histologically confirmed spontaneous true superficial temporal artery aneurysm

Author (Year)	Age (yrs)	Sex	Symptoms and signs	Location of aneurysm	Diagnosis	Size of aneurysm (mm)	Treatment	Outcome
Brown (1942)[1]	34	M	pulsatile mass	preauricular	physical examination	32 × 21 × 21	surgical excision	excellent
Martin and Shoemaker (1955)[9]	60	M	pulsatile mass	frontal branch	physical examination	not described	surgical excision	excellent
Buckspan and Rees (1986)[2]	70	M	pulsatile mass	preauricular	angiography	30 × 40	surgical excision	excellent
Locatelli et al. (1988)[7]	10	M	pulsatile mass	parietal branch	angiography	10 × 40	surgical excision	excellent
Nishioka et al. (1988)[10]	14	M	pulsatile mass	parietal branch	angiography	15 × 10	surgical excision	excellent
Endo et al. (2000)[5]	85	M	two pulsatile masses	preauricular and frontal branch	angiography	30 × 30, 10 × 10	surgical excision	excellent
Porcellini et al. (2001)[12]	24	F	pulsatile mass	parietal branch	physical examination	not described	surgical excision	excellent
Present case	78	F	pulsatile mass	preauricular	3D CT angiography	47 × 45 × 35	surgical excision	excellent

3D CT: three-dimensional computed tomography.

the present case (Table 1).[1,2,5,7,9,10,12] The 6 male and 2 female patients were aged between 10 and 85 years old. The aneurysm arose in the main trunk of STA in 4 cases and in the distal branch of STA in 4. All patients safely underwent surgical excision. The age range suggests that atherosclerosis is not the common and only cause, although atherosclerotic change of the STA and/or hemodynamic stress to the arterial wall might be important in its development.[5] Congenital vulnerabilities of the arterial wall, such as defect of the elastic membrane, may contribute to the development of a true STA aneurysm.[10] In the present case, both aneurysm and scalp tumor simultaneously increased in size for about 2 years. Therefore, we speculate that increased blood supply to the scalp tumor may have caused hemodynamic stress in the proximal STA and promoted the unusual growth of the aneurysm. The histological findings in the present case support this mechanism (Fig. 4). Three previous cases of giant true STA aneurysm of more than 25 mm of diameter have been reported.[1,2,5] All cases were located in the preauricular region, as in the present case. The aneurysm size varied from 30 to 40 mm.

Spontaneous true STA aneurysm usually occurs as a pulsatile scalp mass (Table 1). Any pulsatile, preauricular mass requires careful diagnosis. STA aneurysms often display arterial pulsation and thrills corresponding to systole, whereas STA arteriovenous fistula displays continuous thrill and bruit.[11,12,14] The differential diagnosis also includes aneurysm of the middle meningeal artery with temporal bone erosion, abscess, inflammatory lesion, epidermal inclusion cyst, angiofibroma, meningocele, encephalocele, parotid tumor, and lipoma.[3,11,14]

Cerebral angiography is the gold standard for diagnosis of spontaneous true STA aneurysm.[2,5,7,10,11] In the present case, MR imaging and ultrasonography were useful to visualize the turbulent flow within the aneurysm. Recent developments of multi-detector CT can non-invasively visualize intra- and extracranial vascular lesions with high spatial resolution.[6] Especially in the present case, 3D CT angiography provided important information on the anatomical relationship between the aneurysm and the surrounding tissue, including the external auditory meatus and zygomatic arch. Furthermore, 3D CT angiography could clearly visualize the topographical relationship between the aneurysm and the proximal STA. Based on the findings, we could avoid intraoperative massive bleeding by ligating the proximal STA.

The natural history of spontaneous true STA aneurysm is not well documented. However, we selected surgical resection because the giant aneurysm had gradually increased in size to almost obstruct the left external auditory meatus. Although local anesthesia is preferred for surgical excision, the aneurysm was resected under general anesthesia because of the large size and apparent location near the facial nerve.[8] STA aneurysm in the preauricular region should carefully be dissected from the surrounding tissue to avoid postoperative facial nerve paresis.

References

1) Brown RK: Aneurysm of the temporal artery. *Surgery* 12: 711–715, 1942
2) Buckspan RJ, Rees RS: Aneurysm of the superficial temporal artery presenting as a parotid mass. *Plast*

Reconstr Surg 78: 515–517, 1986

3) Cheng CA, Southwick EG, Lewis EC 2nd: Aneurysms of the superficial temporal artery: literature review and case reports. *Ann Plast Surg* 40: 668–671, 1998

4) DeSanti L: Des tumeurs anev. dela region temporale. *Arch Gen Med* 154: 543, 679, 1884 (Fre)

5) Endo T, Mori K, Maeda M: Multiple arteriosclerotic fusiform aneurysms of the superficial temporal artery—case report. *Neurol Med Chir (Tokyo)* 40: 321–323, 2000

6) Higashino T, Kawashima M, Mannoji H: Three-dimensional computed tomography angiography for the investigation of superficial temporal artery pseudoaneurysms—two case reports. *Neurol Med Chir (Tokyo)* 45: 152–155, 2005

7) Locatelli D, Messina AL, Ricevuti G, Gajno TM: Superficial temporal artery aneurysms. *J Neuroradiol* 15: 89–93, 1988

8) Lozman H, Nussbaum M: Aneurysm of the superficial temporal artery. *Am J Otolaryngol* 3: 376–378, 1982

9) Martin WL, Shoemaker WC: Temporal artery aneurysm. *Am J Surg* 89: 700–702, 1955

10) Nishioka T, Kondo A, Aoyama I, Nin K, Shimotake K, Tashiro H, Takahashi J, Kusaka H: [A case of spontaneous superficial temporal artery aneurysm]. *No Shinkei Geka* 16: 1009–1012, 1988 (Jpn)

11) Peick AL, Nichols WK, Curtis JJ, Silver D: Aneurysms and pseudoaneurysms of the superficial temporal artery caused by trauma. *J Vasc Surg* 8: 606–610, 1988

12) Porcellini M, Bernardo B, Spinetti F, Carbone F: Outpatient management of superficial temporal artery aneurysms. *J Cardiovasc Surg (Torino)* 42: 233–236, 2001

13) Romero AC, Fulkerson E, Rockman CB, Bosco J, Rosen J: Traumatic superficial temporal artery pseudoaneurysms in a minor league baseball player: a case report and review of the literature. *Am J Orthop* 33: 200–205, 2004

14) Schechter MM, Gutstein RA: Aneurysms and arteriovenous fistulas of the superficial temporal vessels. *Radiology* 97: 549–557, 1970

15) Winslow N: Aneurysm of the temporal artery. *Surgery* 28: 696–702, 1935

Address reprint requests to: Masahito Kawabori, M.D., Department of Neurosurgery, Hokkaido University Graduate School of Medicine, North 15 West 7, Kita-ku, Sapporo 060-8638, Japan.
e-mail: masahitokawabori@yahoo.co.jp